

Enhancing Energy Resolution and Particle Identification via Chromatic Calorimetry: A Concept Validation Study

Devanshi Arora^{1,2,*}, Matteo Salomoni^{1,3}, Yacine Haddad⁴, Isabel Frank^{1,5}, Loris Martinazzoli^{1,3}, Marco Pizzichemi^{1,3}, Michael Doser¹, Masaki Owari², Etienne Auffray¹

¹European Organization for Nuclear Research (CERN), Geneva, Switzerland

²Shizuoka University, Hamamatsu, Japan

³University of Milano-Bicocca, Piazza dell'Ateneo Nuovo, 1, 20126 Milan, Italy

⁴Northeastern University, Boston, USA

⁵Ludwig Maximilian University of Munich, Munich, Germany

Abstract. In particle physics, homogeneous calorimeters are used to measure the energy of particles as they interact with the detector material. Although not as precise as trackers or muon detectors, these calorimeters provide valuable insights into the properties of particles by analyzing their energy deposition patterns. Recent advances in material science, notably in nanomaterial scintillators with tunable emission bandwidths, have led to the proposal of the chromatic calorimetry concept. This proposed concept aims to track electromagnetic or hadronic shower progression within a module, enhancing particle identification and energy resolution by layering scintillators with different emission wavelengths. The idea is to use the emission spectra of the inorganic scintillators to reconstruct the shower progression. Our study validates this proposed concept using inorganic scintillators strategically stacked by decreasing emission wavelength. Using electrons and pions with up to 100 GeV, we achieved analytical discrimination and longitudinal shower measurement. This proof of concept underscores chromatic calorimetry's potential for broader applications.

1 Introduction

In particle physics experiments, it is essential to understand the longitudinal evolution of particle showers to identify and characterize incoming particles accurately and to study their interactions with matter. Measuring particle shower profiles in calorimeters plays a vital role in this process. Homogeneous calorimeters, however, lack longitudinal segmentation, making it difficult to obtain detailed information about the shower development along the particle's path. Recent developments in nanomaterial scintillators have the potential for significant applications in particle physics due to their unique optical and electronic properties [1, 2]. These nanoscale semiconductors exhibit size-tunable emission spectra, high photostability, and brightness, making them highly suitable for advanced detection techniques in calorimetry. The tunable optical properties of quantum dots [3] allow for better integration into different materials and environments, enhancing their compatibility with other detection system components. These advancements position quantum dots as a pivotal technology in developing next-generation calorimeters for particle physics research. Hence, these advances in the tunability and narrow emission bandwidth (~20 nm) of quantum wells, carbonized polymer dots, monolayer assemblies, and perovskite nanocrystals enable a new method for measuring the progression of electromagnetic or hadronic showers along a scintillator. This approach offers the potential for longitudinal tomography of the shower profile using a single monolithic device through chromatic calorimetry [4].

Chromatic calorimetry represents an innovative approach aimed at enhancing the precision and capabilities of traditional homogeneous calorimeters. This study presents a proof-of-concept device featuring various layers of inor-

ganic scintillating materials with different emission wavelengths. These materials are stacked in the order of decreasing emission wavelengths, with the shortest wavelength positioned at the end of the device. This arrangement enables one-directional transparency, as illustrated in Fig. 1.

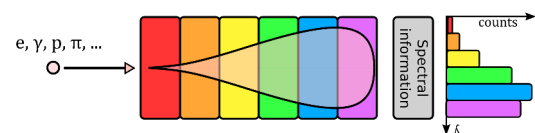


Figure 1. Chromatic calorimetry concept: Particle type and energy information can be enhanced by associating each wavelength with a specific longitudinal segment of the calorimeter (modified from [4]).

2 Materials and methods

The crystal stack was constructed using the following inorganic scintillators, shown in Fig. 2 (the last dimension is along the longitudinal shower propagation): 1x2x2 cm³ gadolinium aluminum gallium garnet (GAGG, 540 nm peak emission), 2x2x5 cm³ and 2x2x12 cm³ lead tungstate (PWO, 420 nm peak emission), 2x2x3 cm³ bismuth germanate (BGO, 480 nm peak emission), and 2x2x2 cm³ lutetium yttrium oxy orthosilicate (LYSO, 420 nm peak emission). This scheme was designed to obtain scintillation light from 3 crystals: at the beginning of the shower (in GAGG), in the shower maximum (in BGO), and at the end of the shower (in LYSO). The experimental scheme was completed with a Hamamatsu Multi-anode Photo-multiplier tube (MaPMT) readout system [5], which selected the emission characteristics of the light emitted at different depths of the shower, thanks to different optical filters (1 per emission of crystal) placed in front of the three out 4 photo-cathode of the PMT, the

*e-mail: devanshi.arora@cern.ch

fourth photo-cathode reading all the signals. PWO crystals, used for their high density and transparency to the emission wavelengths of the other crystals, are integrated within the stack to allow for shower development between GaGG, BGO, and LYSO. The integration of PWO crystals into the stack serves a dual purpose, PWO's high density allows for effective photon absorption. It minimizes re-absorption losses from other scintillators, and by placing one PWO crystal towards the beginning and the end of the stack, we can capture scintillation light generated throughout the entire shower development process. The order of the crystal along the shower propagation was chosen to mitigate re-absorption effects, ensuring efficient photon transmission throughout the stack. PWO is primarily used in our design for its high density and transparency to the emission wavelengths of other scintillators. However, it is not considered an ideal absorber for our measurements. The emission spectrum of PWO peaks around 420 nm, which overlaps with that of LYSO. The configuration of our chromatic calorimeter stack includes two lead tungstate (PWO) crystals, but reading both separately may not provide significant advantages for our measurements. Although PWO is a high-density material, its light yield is considerably lower than that of dedicated scintillators such as LYSO. Specifically, the light output of LYSO is approximately 200 times greater than that of PWO, with LYSO producing around 30,000–33,000 photons per MeV compared to PWO's much lower output [6]. Thus, reading both PWO crystals separately is not beneficial because the significantly lower light yield of PWO compared to LYSO means that the MaPMT signal is predominantly influenced by LYSO, overshadowing any contributions from the PWO crystals. We measured energy deposition and photon yield across all output channels using data analysis and Geant4 simulations [7]. These measurements offer valuable insights into the calorimeter's response and the behavior of electromagnetic showers. Our study emphasizes electron-pion discrimination, profiling the shower along its length, and the relationship between energy deposition and the measured amplitude in three different spectral channels. This highlights the need for precise detector design adjustments to improve the effectiveness of chromatic reconstruction.

2.1 Test Beam Setup

The tested chromatic calorimeter module was placed in the experimental box and exposed to a beam of electrons or pions of up to 100 GeV, (see Fig. 3). The Test beam experiment was performed at the Super Proton Synchrotron (SPS) facility in the zone H2/H6 Northern area of CERN in June 2023 [9].

3 Results

3.1 Study of longitudinal shower profile

From the test beam analysis, output signal amplitudes from various channels of the MaPMT at electron beam

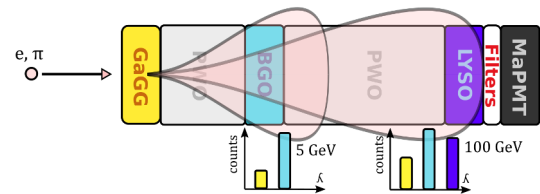


Figure 2. Chromatic calorimeter module schematic: The module comprises inorganic scintillators, read out by a MaPMT with four channels. Three different optical filters are used for three channels of the MaPMT: Thorlabs long pass FELH0550 for GAGG, short pass FESH0450 for LYSO, and bandpass FB490-10 for BGO [8]. The two histograms display the count number for each scintillator relative to particle penetration depth.

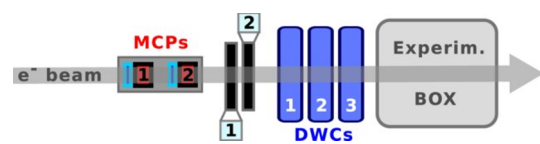


Figure 3. Test beam configuration: The electron beam travels from left to right. Two MCPs (Micro-channel Plates) establish the time reference, while two scintillating pads generate the trigger signal. Three Drift Wire Chambers (DWC) supply the tracking information used for the module alignment. The experimental box houses the prototype and the rotating stepper motors (from [10]).

energies of 25, 50, and 100 GeV were measured, where channels 1, 2, and 4 tuned to the peak emission from BGO, GAGG, and LYSO, respectively using optical filters. Channel 3 is an additional channel that serves as a "neutral" or "no filter" channel. The measured amplitude spectra for 100 GeV electron beam are shown in Fig. 4. In this plot, we can see a clear chromatic separation between different channels. As the energy of the electron beam increases, the signals from other channels become more distinct. This separation helps us accurately identify the incoming particles' energy level. Fig. 5 illustrates the mean output amplitude for channels 1, 2, and 4 at the same energies (25, 50, and 100 GeV). The mean is determined by fitting the channel amplitude using a Crystal Ball function [11], which helps to account for the exponential tails. By averaging the signals from these channels, we can see how they respond to changes in energy. The differences in the average amplitudes reinforce the idea of chromatic separation. In Fig. 6, the plot illustrates how much energy is deposited in each layer of the chromatic calorimeter module, as simulated using Geant4. This plot helps us understand how different materials (like GAGG, PWO, BGO, and LYSO) interact with the incoming particles. The amount of energy deposited in each layer affects the signals we get from the MaPMT, linking back to the amplitude spectra we observed in Fig. 5.

3.2 Electron-Pion Separation

It was observed that exposing the stack with high-energy electrons or pions at the SPS facility, up to 100 GeV, leads

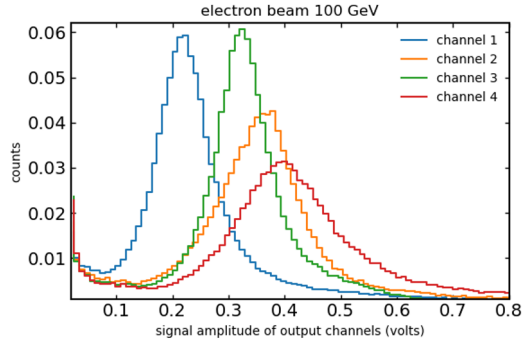


Figure 4. Plot illustrating the output signal amplitude measured by the four output channels of MaPMT for 100 GeV electrons, where channels 1, 2, 3, and 4 correspond to the average signal amplitude response from BGO, GAGG, Neutral, and LYSO, respectively.

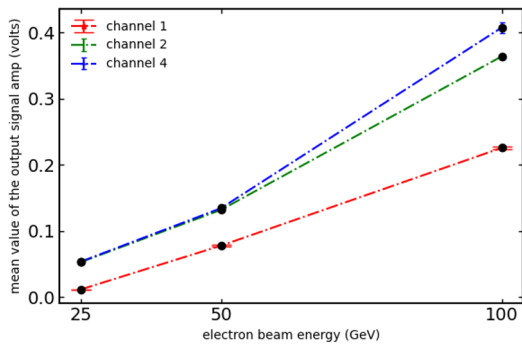


Figure 5. The plot illustrates the mean output signal amplitude across three output channels as a function of different electron beam energies. Channels 1, 2, and 4 correspond to average signal amplitude responses from BGO, GAGG, and LYSO respectively. The curve represents results derived from crystal-ball fitting equations.

to a change in the amplitude ratio between the crystal responses of GAGG, PWO, BGO, and LYSO. This shift allowed us to distinguish electrons from pions (see Fig. 7). A similar amplitude scatter plot can be produced for different energies of the same particle.

In summary, this prototype, which combines various scintillating crystals with a spectral-sensitive readout scheme (comprising a MaPMT and optical filters), provides an insight into the energy deposited in each sampling layer. A distinct chromatic separation between channels was observed at higher electron beam energies. The mean output amplitudes further confirm this separation, supporting the idea that the electromagnetic shower penetrates deeper into the scintillating material at high energies. However, at lower energies, the separation is less pronounced.

In our analysis of electron and pion events using the chromatic calorimeter stack, we conducted measurements without formal calibration of the MaPMT. While calibration is typically a critical step for achieving absolute energy measurements, our primary objective was to evaluate the relative performance of the MaPMT in distinguishing between hadronic and electromagnetic interactions. The clear analytical discrimination observed be-

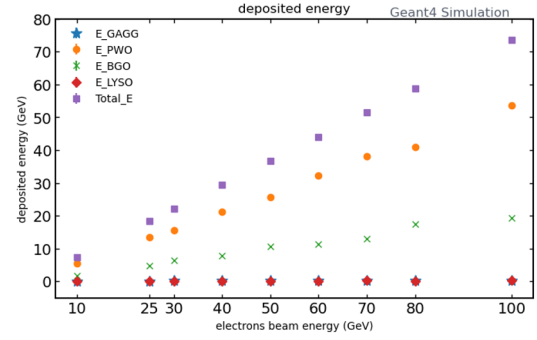


Figure 6. Plot showcasing the energy deposited in a calorimeter module composed of GAGG, PWO, BGO, and LYSO materials, as simulated using Geant4 to electron beam energies ranging from 20 to 100 GeV. Here, E_{GAGG} is the energy deposited in GAGG and so on.

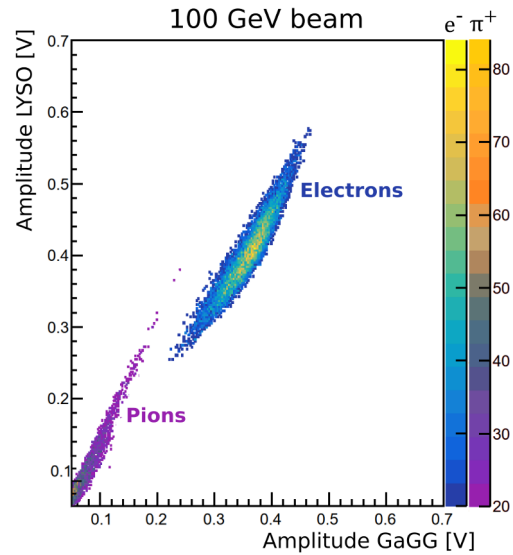


Figure 7. Scatter plots display the correlation between signal amplitudes recorded in GAGG and LYSO for electrons (e^-) and charged pions (π^+) at 100 GeV. Each point corresponds to an event, with the x-axis representing the signal amplitude in GAGG and the y-axis representing the signal amplitude in LYSO. Only events with a bin count exceeding 20 are shown.

tween these particle types (refer Fig 6), as well as the distinct evolution of energy signals concerning incoming particle energy, demonstrates the effectiveness of our reconstruction method despite the lack of calibration. The absence of calibration means that while we can confidently discuss the relative separability and resolution achieved at various energies, we cannot provide precise quantitative energy values. Instead, our findings highlight qualitative trends that indicate how well our setup can differentiate between particles based on their unique energy deposition patterns. The reduced chromatic separation at lower energies, attributed to factors such as suboptimal geometry and spectral contamination from PWO crystals, further emphasizes the need for a refined design in future experiments. Additionally, the limited number of high-energy runs available during this initial validation phase restricted

our ability to perform a comprehensive calibration. We recognize that implementing a calibration procedure will enhance measurement accuracy. Our ongoing research addresses these limitations by optimizing the experimental setup and incorporating advanced materials with well-defined optical properties. These materials will be tested in upcoming beam tests at the SPS facility. We plan to focus on calibrating our system using minimum ionizing particles (MIPs) such as muons.

4 Discussion, conclusion, and outlook

The test beam analysis demonstrates clear analytical discrimination between electron and pion events. The reconstructed energy signals also reveal valuable separability between hadronic and electromagnetic interactions at higher energies, enhancing our ability to differentiate between these events. Additionally, the signals exhibit a distinct evolution concerning the incoming particle's energy, indicating improved resolution and sensitivity across various energies. These observations highlight the effectiveness of the reconstruction method and its potential for precise event classification. Chromatic calorimetry aims to capture detailed information on how energy is deposited along the length of a particle shower. The findings demonstrate that a simple arrangement of different types of inorganic scintillators can effectively distinguish between electrons and pions of identical energy levels. This capability comes from the distinct patterns of energy deposition characteristic of each type of particle. However, the experimental setup has revealed some drawbacks. Specifically, the reduced chromatic separation at lower energies can be attributed to two primary factors. First, the geometry of the current prototype is not optimized for clear separation at the shower maximum. Second, the presence of PWO crystals at the front and rear of the module contaminates the spectra from the GAGG and BGO layers. This contamination reduces the effectiveness of chromatic separation and highlights the need for a more refined design. To address these drawbacks, an optimal setup should employ materials with well-defined emission and absorption spectra, ensuring that each layer contributes uniquely to the detection process. This improved setup is currently under study.

The goal of chromatic calorimetry is to leverage nanomaterials like perovskite and CdSe quantum dots embedded in scintillators with a calorimeter module. With tunable and narrow optical emissions, these materials offer precise control over photon emission, addressing the abovementioned limitations. The approach aims to achieve a more refined longitudinal tomography of electromagnetic showers.

5 Author Contributions

All authors contributed to the paper by providing insight into different sections and correcting the complete document. D.A., E.A., and M.S. planned the design. D.A. performed the data analysis under technical support from Y.H. and M.S. D.A., I.F., L.M., and M.S. conducted the

test beam experiment. E.A., M.D., Y.H., M.O., and M.S. guided and supervised the project.

6 Acknowledgement

This work was carried out in the frame of the CERN Quantum Technology Initiative (QTI) and the CERN Crystal Clear Collaboration (CCC). It is also a part of the ECFA-DRD5 collaboration.

References

- [1] Létant, SE and Wang, T-F, Semiconductor quantum dot scintillation under γ -ray irradiation. *Nano Letters* **6**, 2877–2880 (2006). <https://doi.org/10.1021/nl0620942>
- [2] Zhang, C., et al. Narrow-band violet-light-emitting diodes based on stable cesium lead chloride perovskite nanocrystals. *ACS Energy Letters* **6**(10), 3545–3554 (2021). <https://doi.org/10.1021/acscenergylett.1c02084>
- [3] Liu, Y., et al., Advances in carbon dots: from the perspective of traditional quantum dots. *Mater. Chem. Front.* **4**, 1586–1613 (2020). <http://dx.doi.org/10.1039/DOQM00090F>
- [4] Doser, M., Auffray, E., et al. Quantum Systems for Enhanced High Energy Particle Physics Detectors. *Frontiers in Physics* **10** (2022). <https://www.frontiersin.org/articles/10.3389/fphy.2022.887738>
- [5] Hamamatsu Photonics K.K. (Hamamatsu Hotonikusu Kabushiki-Kaisha). **Photomultiplier tube, R7600U-200**. https://www.hamamatsu.com/us/en/product/optical-sensors/pmt/pmt_tube-alone/metal-package-type/R7600U-200.html
- [6] Mao, R., et al. **Gamma ray induced radiation damage in PWO and LSO/LYSO crystals**. In *2009 IEEE Nuclear Science Symposium Conference Record (NSS/MIC)*, pp. 2045-2049, Orlando, FL, USA, 2009. doi: 10.1109/NSSMIC.2009.5402126.
- [7] Allison, J., et al. (2006). Geant4 developments and applications. **IEEE Transactions on Nuclear Science*, 53*(1), 270-278. <https://doi.org/10.1109/TNS.2006.869826>.
- [8] Thorlabs, Inc. **Spectral Filters**. https://www.thorlabs.com/navigation.cfm?guide_id=2210
- [9] CERN, The European Organization for Nuclear Research. **Secondary Beams and Areas**. <https://sba.web.cern.ch/sba/Documentations/How2controlNAbeams.htm>
- [10] An, L., et al, Performance of a spaghetti calorimeter prototype with tungsten absorber and garnet crystal fibers. **1045**, 167629 (2022). <https://doi.org/10.1016/j.nima.2022.167629>
- [11] Gaiser, J. E. (1982). **Charmonium Spectroscopy From Radiative Decays of the J/ψ and ψ' ** (SLAC-0255, UMI-83-14449-MC, SLAC-R-0255, SLAC-R-255).